FINAL REPORT

STUDY OF THE EFFECTS OF IMPLANTATION ON THE HIGH TEMPERATURE CORROSION AND HYDROGEN PERMEABILITY OF Fe-Ni-Cr AND Ni-Cr-Al ALLOYS

Under Grant No. NAG3-255

M.W. Ribarsky
Principal Investigator
School of Physics
Georgia Institute of Technology

April 12, 1985

TABLE OF CONTENTS

Abstract

A theoretical study of the effects of implantation on the corrosion resistance of Fe-Ni-Cr and Ni-Cr-Al alloys was undertaken. The purpose was to elucidate the process by which corrosion scales form on alloy surfaces. Since the corrosion process is complicated with different mechanisms of scale formations for different materials and with different implants producing varying effects, the theoretical work was carried out in conjunction with experimental analysis. The experiments dealt with Ni implanted with Al, exposed to S at high temperatures, and then analyzed using scanning electron microscopy, scanning Auger spectroscopy and X-ray flourescence spectroscopy. A variety of theoretical approaches were used. Pair bonding and tight-binding models were developed to study the compositions of the alloys, and as a result, a new surface ordering effect was found which may exist in certain real alloys. With these models, the behavior of alloy constituents in the presence of surface concentrations of O or S was also studied. Improvements of the models to take into account the important effects of long- and short-range ordering were considered. The diffusion kinetics of implant profiles at various temperatures were investigated, and it was found that significant non-equilibrium changes in the profiles can take place which may affect the implants' performance in the presence of surface contaminants. Finally, another approach was considered in which molecular cluster calculations would be used to simulate the effect of impurity atoms on the electronic structure at grain boundaries.

I. Introduction

The problem of corrosion of iron and nickel based alloys has been studied extensively. The most successful studies are those which have used a combination of techniques such as scanning electron microscopy, Auger analysis, x-ray diffraction and emission, sputter profiling, marker experiments and other techniques to provide information about the structure, composition and morphology of the scales formed, and about the diffusion rates and paths of the constituents. Only with combinations of techniques such as these can one reach definite conclusions about the complicated corrosion processes which occur especially in alloys with more than two components or with impurities. Unfortunately, there has not been much basic theoretical analysis in conjunction with most of these experimental results. Such an analysis is necessary if one is to understand the basis of the competing corrosion mechanisms and the process by which the ions arrive to form the scale, and especially if one is to predict the effect of various additions to the alloy. The purpose of this work was to provide some of this theoretical analysis.

Resistance to metallic corrosion can also be improved by ion implantation. Among the qualities of ion implantation is that relatively small amounts of scarce or expensive elements can be implanted and can provide materials behavior quite similar to that of bulk alloys. The elements can be implanted in controlled amounts and distributions and at non-equilibrium concentrations far greater than in the alloying process so that new materials may be formed. However, due to the nature of the implantation process, one must be aware of possible differences in diffusion rates or structure caused by radiation damage or non-equilibrium concentrations. For example, Fe-Ni-Cr-Al alloys have been formed by implanting Ni, Cr and Al in Fe[1] and these provide corrosion resistance similar to the bulk alloys. However, sputter profiling with proton-induced x-rays showed a diffusion rate of Al in Fe at 300°C which was 9 orders of magnitude greater than the volume diffusion rate! The difference may have been due to radiation-enhanced diffusion, but there was not much difference

between the bulk and implanted diffusion rates in the Cr and Ni implanted alloys. The nature of the oxide or other scale formed on the implanted material can also be significantly different than on the unimplanted material and quite dependent on the implanted species. All this makes a careful analysis of the corrosion process for each implanted material highly useful, especially since there have been few such studies.

It is well known that alloys of iron or nickel with 20 wt% or more chromium form continuous Cr_2O_3 scales when oxidized. In Ni-Cr or Fe-Ni-Cr alloys, the Cr_2O_3 scales provide good resistance to further high temperature oxidation when they are adherent, but they are permeable to sulfur and sulfur-bearing species which lead to base metal corrosion. Additions of certain elements, sometimes in small amounts, can greatly improve the resistance of the oxide to corrosion or sulfidation or can increase the adherence and stability of the scale. Ion implantation can be of great use in adding these elements to the surface region without changing the bulk properties.

The addition of several percent Al to the Fe-Cr and Ni-Cr alloys forms a surface oxide mainly consisting of Al_2O_3. The Al_2O_3 scale provides greater protection than the Cr_2O_3 scale but spalls at high temperatures. Relatively minor additions of rare earths such as Ce or transition metals such as Y or Sc greatly improve the oxidation resistance of the Al-doped alloys. Voids form in the undoped Fe alloys which are connected with the Al_2O_3 scale which grows at the grain boundaries. Additions of Ce migrate to the grain boundaries and prevent void formation by capturing vacancies.[2] The result is a significant improvement in oxide adherence. The mechanism of void formation is similar for Ni-Cr-Al alloys.[3]

II. Interactions, Talks and Papers

During the course of this research, there have been several interactions and communications with researchers and also talks given and papers presented. Abstracts for the main papers are in the Appendix.

The main interactions have been with:

- Dr. Keith Legg of the School of Physics at Georgia Tech concerning the implanting and analysis of Ni alloys,
- Dr. Susan Schuon at NASA-Lewis concerning the results of the calculations and analyses,
- Dr. Susan Benford of NASA-Lewis concerning the nature and scope of this research program.

Talks presented on this work include the following colloquia:

- "Effects of Implantation on the Corrosion Properties of Iron and Nickel Alloys," presented at NASA-Lewis in August, 1982;
- "Surface and Grain Boundary Segregation in Alloys," presented at the School of Physics, Georgia Tech in November, 1982.

The following papers have been produced on this work:

- "Surface Segregation in Ternary Alloys," 42nd Physical Electronics Conference, Atlanta, Georgia (1982);
- "The Diffusion of Implanted Ions Near Surface and Grain Boundaries," Bull. Amer. Phys. Soc. 29, 389 (1983).

The following article is in preparation:

- "Effects of Temperature and Surface Contamination on the Diffusion of Implanted Ions."

III. Models of Segregation in Binary and Ternary Alloys

We have made considerable progress in extending segregation models to ternary systems. The extension involves minimizing the free energy. $F(X_1^A, X_1^B, \ldots X_2^A, X_2^B \ldots)$ with respect to concentrations of each species in the first, second, etc... crystal layers parallel to the surface. Under the constraint that the total number of atoms of each species remains fixed, the minimization condition is

$$\frac{\partial F}{\partial X_i^\alpha} = \frac{\partial F}{\partial X_B^\alpha} \qquad \begin{matrix} i = 1, 2, 3. \ldots \\ \alpha = A, B, C, \ldots \end{matrix} \tag{1}$$

where X_i^α is the concentration of species α in the i'th layer and X_B^α is the bulk concentration.

We are using two models in evaluating Eq. (1): a tight-binding method and a pair-bonding method.[4,5] In the latter method, one assumes that only the nearest neighbor interactions contribute and derives bond enthalpies H_{AA} for identical atoms from the heats of vaporization of the pure elements. One then uses heat of mixing data or interaction calculations[6] to derive the bond enthalpy H_{AB} between different atoms. For a random binary system the resulting internal energy contribution from atoms in the first layer is

$$U_{11} = -Z_\ell \left[\frac{1}{2} X_1^2 H_{AA} + X_1(1-X_1) H_{AB} + \frac{1}{2} (1-X_1)^2 H_{BB} \right] \tag{2}$$

where Z_ℓ is the number of nearest neighbors for that layer. Similar equations hold for U_{12}, U_{22}, U_{23} and so on and for the general case of multicomponent systems.

A. Surface Segregation in the Pair-Bonding Model

We have studied the general behavior of the pair-bonding model as the

model parameters are varied and have added effects such as short-range order and elastic mismatch energies for the case when different size components are present. In most cases we find that short-range order effects are fairly small and that the major contribution due to size mismatch is already contained in the heat of mixing term. We also find that, in general, raising the temperature lowers segregation and that one should use surface energies of the components rather than heats of vaporization to calculate the internal energy of the surface layer. Lastly we find a striking dependence on the size and sign of the heat of mixing which we will discuss below.

Our pair-bonding calculations for the (111) surface layer concentration of Cu-Ni are shown in Fig. 1. We chose Cu-Ni as a test system because it has been extensively studied experimentally and theoretically. As can be seen, the calculations are in good agreement with the experimental data[7] and show the correct temperature dependence.

B. Segregation and electronic structure in the tight-binding model

In contrast to the pair-bonding model, the tight-binding model provides a description of the electronic structure at the surface in terms of microscopic quantities such as the band centers and band widths of the pure metals and the interactions between sites as the alloy is formed. The equations are more complicated than in the pair-bonding model and more time-consuming to evaluate because one must calculate densities of states at a range of energies for each set of layer configurations and then numerically integrate over energy to obtain the total free energy. This process must be followed to find each layer concentration by solving Eq. (1), and then the whole procedure must be repeated until the concentrations do not change from one iteration to the next. In spite of the effort necessary, the method yields microscopic information which can be quite valuable in evaluating the chemistry of a surface or grain boundary and in

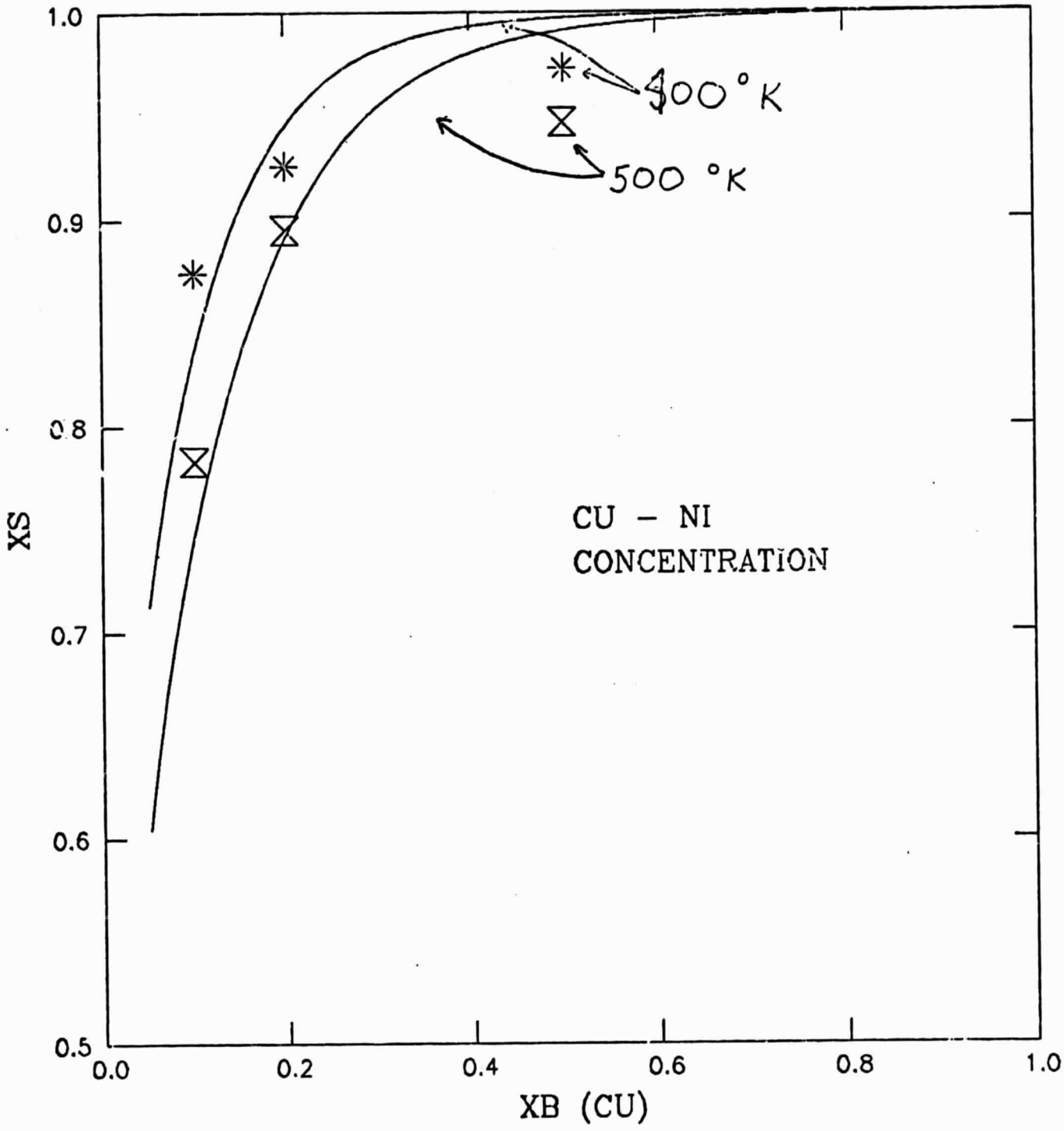

Fig. 1 Comparison of the calculated Cu-Ni concentration at the (III) surface with Low Energy Ion Scattering results (Ref. 4).

studying the effects of impurities or defects.

Our results for the the Cu-Ni binary system are shown in Fig. 2. These results are at 600°K so that the surface segregation of Cu should be somewhat less than the experimental results in Fig. 1. However, the experiments[7] show no tendency to cross over the zero segregation line between 60 and 70 at % Cu as the results in Fig. 2 do. Recent calculations[8] indicate that the additional constraint

$$\frac{\partial F}{\partial \langle n_i \rangle} = \frac{\partial F}{\partial \langle n_b \rangle} \tag{3}$$

when required with Eq. (1) brings the Cu-Ni tight-binding results into excellent agreement with experiment. Here $\langle n_i \rangle$ is the average electron number on an atom in the i'th layer so that Eq. (3) is the requirement that the number of electrons remains fixed.

There has been a good deal of work[9-11] in recent years directed toward understanding the roles of d, s and p valence electrons in the bonding of transition metal alloys and in contributing to the alloy cohesive energies and heats of formation. Relatively simple models have been constructed[10-11] which show that accurate heats of formation can be obtained using rectangular d-band densities of states having the band positions and widths appropriate to the pure metals except for some straightforward modifications due to alloying. Calculations with these models show that the d-bands make the most significant contribution to the heats of formation for transition metals. Since the heats of formation are directly related to the pair bonds in the pair bonding model, this method provides a direct way of evaluating the contributions of electronic structure to the pair bonds. Also the simple modelling of the d-bands in terms of position and width is just the information needed to define the parameters in the tight-binding model. We thus have a method to directly connect the results of the tight-binding and pair-bonding models.

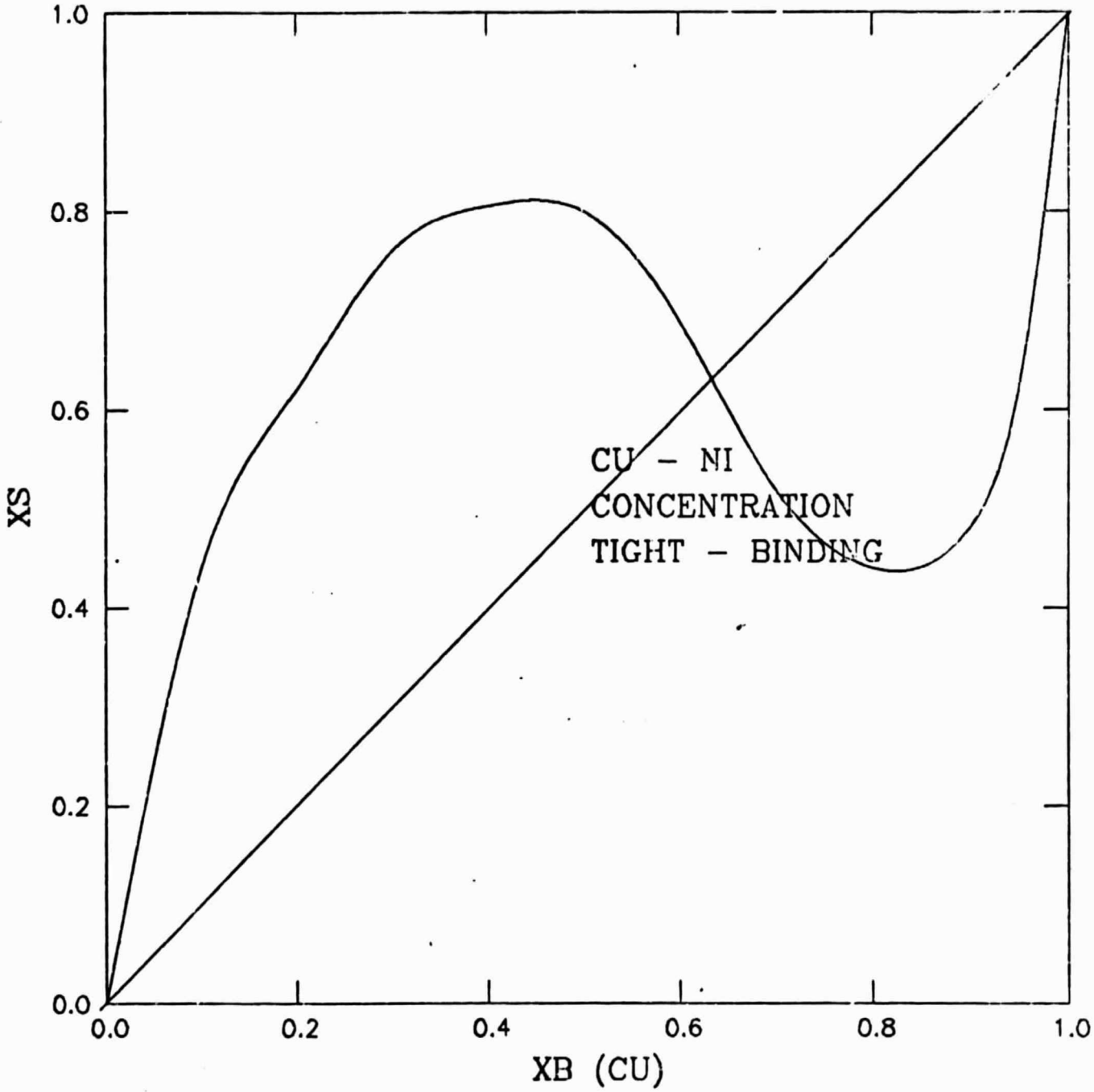

Fig. 2 Tight-binding calculation of Cu-Ni surface concentration At T=600°K.

C. Grain boundary segregation

The composition and structure of grain boundaries greatly affect the strength, oxidation rates and adherence of oxides in polycrystalline materials. In alloys the addition of small amounts of certain metals to the base metal can greatly affect the segregation of trace impurities to the grain boundary and thus change significantly the properties of the system. For example, when Ni is added to Fe, the grain boundary segregation of impurities such as Sn or Sb can be increased by a factor of 15 or 20. The resulting alloy undergoes temper embrittlement and all fractures occur along the grain boundary.

The pair-bonding model is quite successful in explaining this enhancing effect. If one defines the parameter α' as follows,

$$\alpha' = \alpha_{M-I} - \alpha_{M-Fe} - \alpha_{I-Fe} \qquad (4)$$

where α_{M-I} is the interaction strength of the added metal and the trace impurity, then for $\alpha'>0$ the pair-bonding model predicts that the boundary segregation of I will be enhanced by the presence of M[12]. We have found the interactions α_{M-I}, α_{M-Fe} and α_{I-Fe} using experimental heat of solution data, and our results are shown in Table I for the effect of Cr, Ni, V, Mn and Co on Sn and Sb. In every case the predicted enhancement is seen experimentally. When $\alpha'<0$ the model shows depletion of I at the boundary, so that we can also predict which elements will have the opposite effect.

α' VALUES FOR Fe-M-I SYSTEMS

M \ I	Sn	Sb
Ni	4.6 (+)	3.7 (+)
Cr	.35 (+)	1.3 (+)
Mn	6.1 (+)	7.5 (+)
V	4.0 (+)	6.3 (+)
Co	3.3 (+)	

Table I Comparison of α' values with experimental determinations of grain boundary enhancement. The (+) indicates that the M component enhances the segregation of the I component.

IV. Surface Layering Effect and Long- and Short-Range Ordering

Usually the solutions to Eq. (1) return to the bulk concentrations by the fourth or fifth layer. However, in certain cases a remarkable surface layering effect shows up. For example, the layer concentrations for the first 8 layers of Fe (61 at %) - Ni (19 at %) - Y are shown in Fig. 3. The Y does not segregate to the surface layer but segregates strongly to the second layer. However, the first, third, fifth layers and so on are almost entirely Ni while the alternate layers are almost entirely Y. This effect persists much deeper into the bulk than is usually the case. Evidently, the layering effect is related to the large attraction between Y and Ni reflected in their large heat of mixing. The energy is favorable for Ni segregation in the surface layer, but the large attractive interaction causes Y to segregate in the second layer and so on.

Other effects may impair this surface layering effect. In the Fe-Ni-Y system, Y has a much larger volume than Fe or Ni. Thus Y would want to segregate to the surface to reduce lattice strain and therefore the surface layering effect would be diminished. In principle one could diminish this effect by choosing elements which strongly attract but are of similar sizes. However, there are also other ordering effects which could significantly alter the segregation pattern, and we will discuss these next.

The surface layering effect is a type of ordering phenomenon. To get a complete picture, one must also add the effects of bulk and surface short- and long-range ordering. For systems with large heats of mixing between two components, such as is the case for the surface layering effect, some type of long- or short-range ordering becomes more likely. We can introduce ordering by considering a lattice with α and β sublattices. For a BCC crystal, the α sublattice might be the corners and the β sublattice the body-centered sites. For an FCC crystal, the α sublattice might be the face centered sites and β sublattice might be the corners. These types

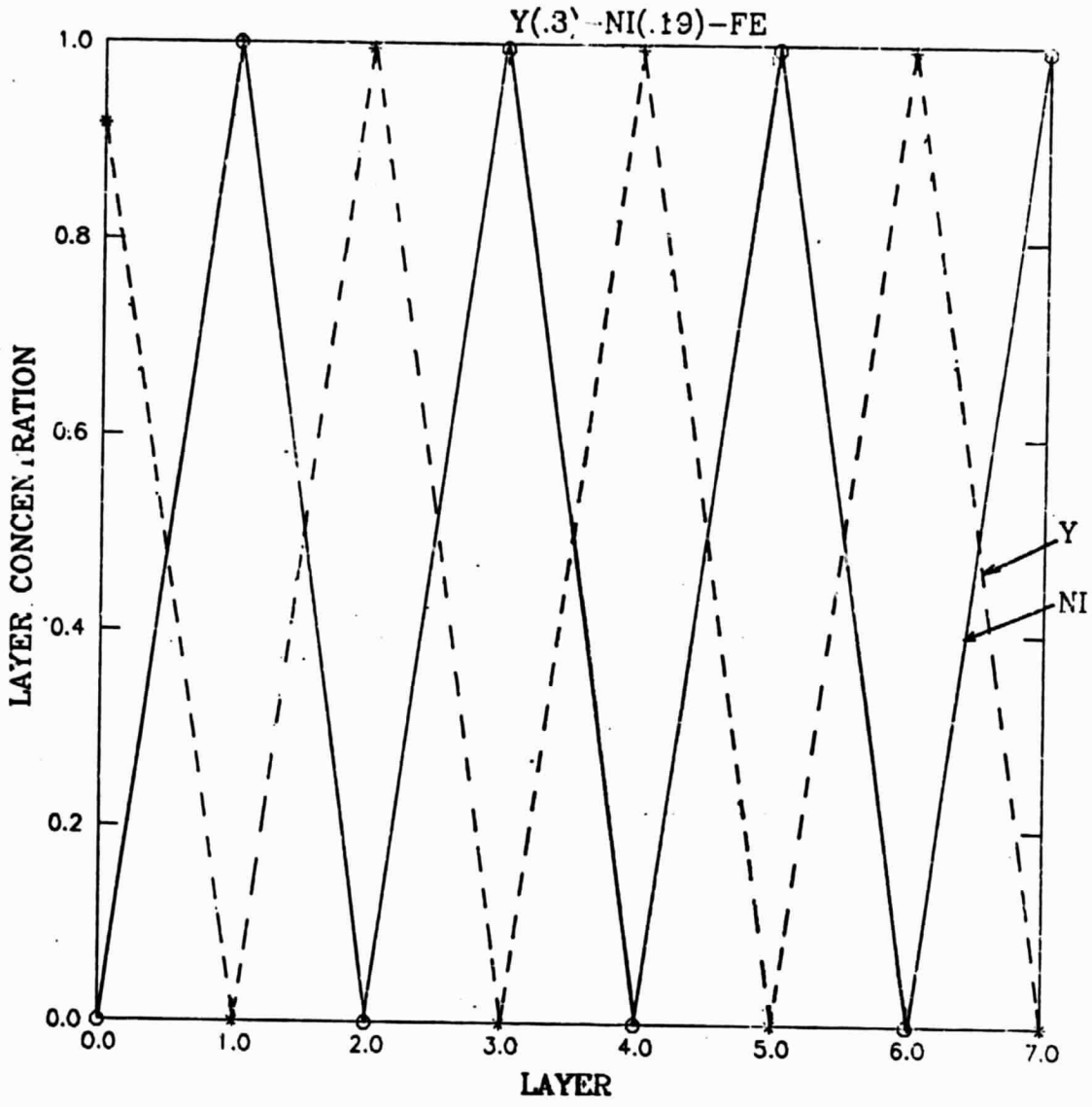

Fig. 3 Concentration of Y and Ni in the first eight layers at T=298^{o}K.

of ordering have been seen for several AB-type alloys in the BCC case and A_3B-type alloys in the FCC case.

We may consider a simple nearest-neighbor-only pair-wise interaction model for our alloy. For a binary system in the bulk, the short- and long-range order parameters are defined in terms of the pair probability $P_{IJ}^{\alpha\beta}$ which is the probability of finding an IJ bond with the I atom in the α sublattice and the J atom in the β sublattice. The pair probabilities are normalized by

$$P_{AA}^{\alpha\beta} + P_{AB}^{\alpha\beta} + P_{BA}^{\alpha\beta} + P_{BB}^{\alpha\beta} = 1 \quad . \tag{3}$$

The long-range order (LRO) parameter is

$$\eta \equiv P_{AB}^{\alpha\beta} - P_{BA}^{\alpha\beta} \tag{4}$$

so that if A is completely ordered on sublattice α and B on sublattice β or vice-versa, then $\eta = \pm 1$. On the other hand, if A and B are random, then $P_{AB}^{\alpha\beta} = P_{BA}^{\alpha\beta}$ and $\eta = 0$. We define the short-range order (SRO) parameter as

$$\sigma \equiv 1 - [(P_{AB}^{\alpha\beta} + P_{BA}^{\alpha\beta})/2x(1 - x)]. \tag{5}.$$

Since for a random system $P_{AB}^{\alpha\beta} = x(1 - x)$, $\sigma = 0$. Now the SRO would be in the form of clustering. In the most ordered state all nearest-neighbors would be alike except at the boundaries $P_{AB}^{\alpha\beta} = P_{BA}^{\alpha\beta} = 0$ so that $\sigma = 1$.

The main difference due to ordering in the expression for the free energy introduced in Eq. 1 is in the entropy term. In the pair approximation,[13] the entropy is

$$S = \kappa N[1/2(Z - 1)\sum_{I,\nu} P_I^{\nu} \ln P_I^{\nu} - 1/2\, Z \sum_{IJ} P_{IJ}^{\alpha\beta} \ln P_{IJ}^{\alpha\beta} \tag{6}$$

where P_I^{ν} is the site probability that atom I is in the ν sublattice. Here N is the total number of sites in the crystal and Z is the number of nearest-neighbors. The

equilibrium values η and σ , for a given concentration x, are obtained by minimizing the free energy F

$$\frac{\partial F}{\partial \sigma} = 0 \quad \frac{\partial F}{\partial \eta} = 0 \quad . \tag{7}$$

With Eq. (3-7) one can find σ and η in terms of x. Similar equations exist for the surface except that η and σ will depend on the surface layer. Also, we can generalize to ternary ABC systems by defining η and σ for AB, AC and BC pairings. Calculations show that LRO effects due to large heats of mixing diminish surface segregation effects.[14] Thus the surface layering effect would be diminished. On the other hand, strong surface segregation also diminishes LRO. Further calculations are necessary to see whether LRO or surface layering wins out.

V. Calculations of Surface and Grain Boundary Composition

The surface or grain boundary is often where the action is in corrosion and embrittling processes. Impurity ions may diffuse mainly along the surface or grain boundary or may segregate significantly to these boundaries. Certain impurities, such as S or P, may segregate strongly to the grain boundary under certain conditions and cause intergranular failure. Other impurities, such as Ce or Y, enhance scale adhesion after segregating to grain boundaries. Of course the scale formations process itself begins in the boundary region and the kinetics of ion diffusion across the boundary determine the structure of the scale as, for example, when inner and outer oxides form due to different diffusion rates of alloy constituents.

In this section we will show that the basic theory can give quite useful qualitative and even quantitative results for the compositions of alloy surfaces and grain boundaries. Thus one can obtain a lot of information about alloy behavior just by comparing the appropriate parameters for different constituents. We will use the basic pair-bonding theory as outlined briefly in Sec. II, but we will ignore the effects of long- and short-range order. The structure of the pair-bonding equations for the grain boundary is nearly the same as for the surface, although grain boundary energies must replace surface energies, and site competition may not be as important at the grain boundary due to lattice distortion.

The effect of oxygen at an alloy surface can be significant. As shown in Figs. 4a and 4b for Ni-Cr-Al alloys of varying compositions, Ni segregates strongly to the clean surface. However when an oxygen mono-layer is added, the Cr is pulled to this surface. The result that the surface concentration of Cr in Fig. 4b is 50% at about 20 at % bulk Cr is in agreement with experiments

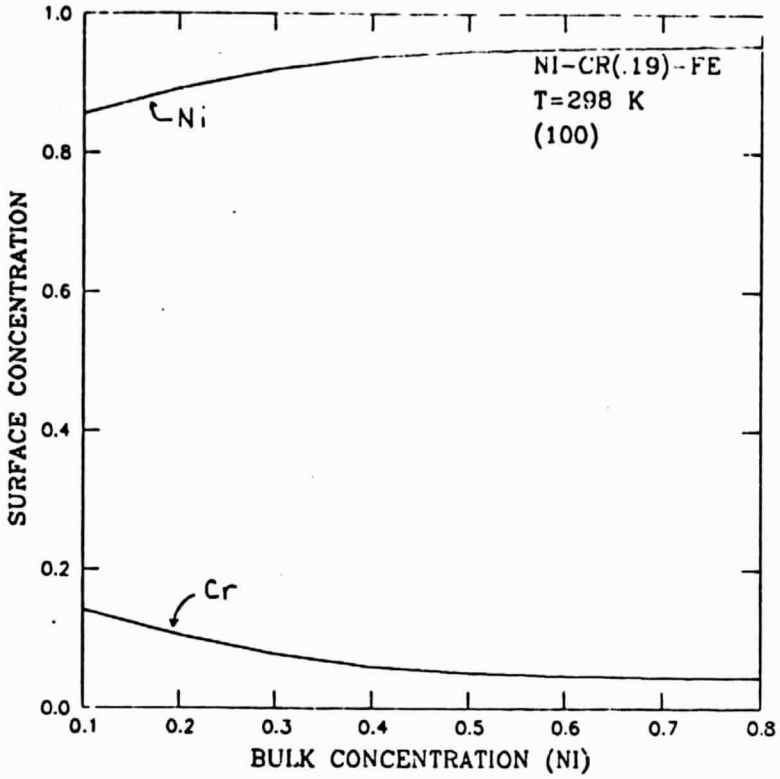

Fig. 4a Ni and Cr surface concentrations for clean Ni-Cr-Fe. The Ni strongly segregates.

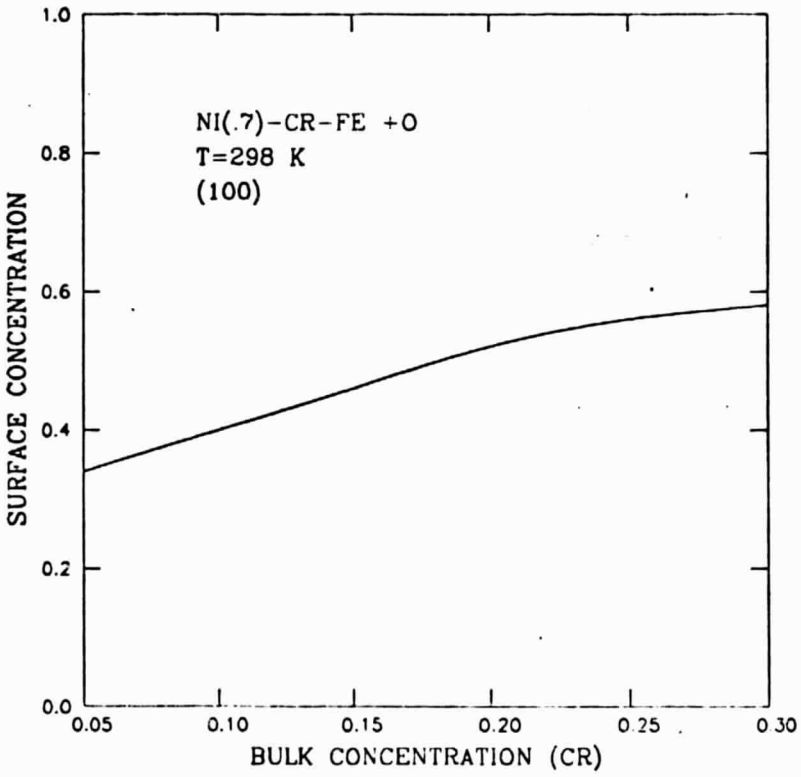

Fig. 4b The dependence of Cr surface concentration on bulk concentration when an oxygen monolayer is added. Note that the surface concentration is 50% at about 20% bulk Cr.

which show a Cr-rich oxide appearing at about 20 at % bulk Cr. If we have an Ni-Cr-Al alloy plus oxygen, on the other hand, the situation is quite different and Al segregates strongly as shown in Fig. 5. This result is in agreement with experiments which show that surface oxides on Fe-Cr-Al alloys with more than 4 at % Al are mostly alumina. The qualitative behavior of segregation with oxygen adsorption is predicted using oxide heat of formation data to estimate the oxygen-metal bond strength. Thus Al is attracted to O more strongly than either Cr or Ni, and the rare earths are attracted even more strongly still. This last result is consistent with the observation of Ce and O at grain boundaries during the initial stages of oxidation in Fe-Cr-Al alloys.[15]

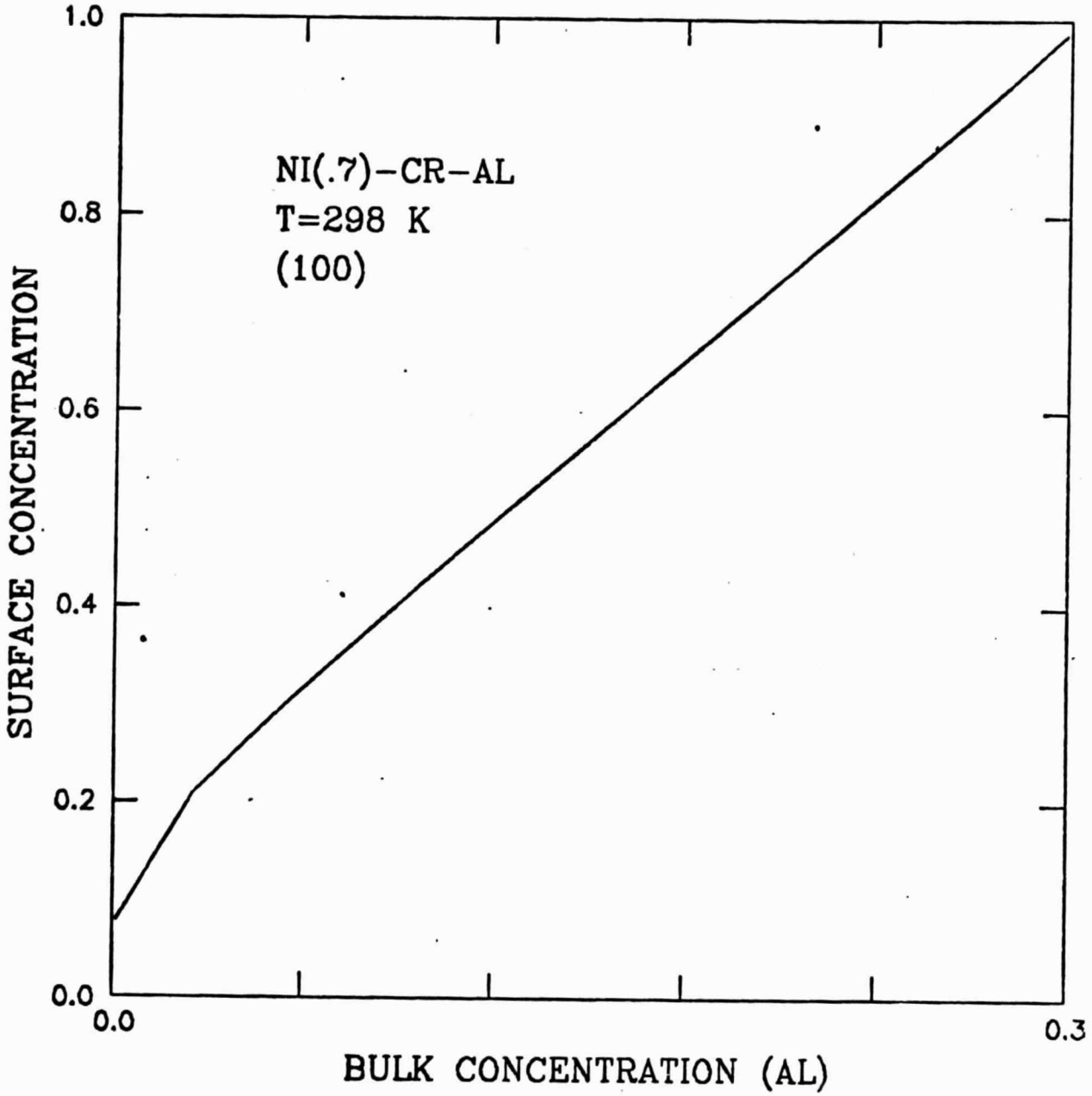

Fig. 5 Al concentration in a Ni(.7)-Cr-Al alloy with a half monolayer of O on the surface. The slope discontinuities are due to a sparse number of points.

VI. Diffusion of Implant Profiles

The time-dependence of the concentration for a binary system in the diffusion approximation can be found by considering the equation [16]

$$\frac{\partial C_b}{\partial t} = \frac{\partial^2 C_b}{\partial x^2} \tag{8}$$

subject to the boundary conditions

$$\frac{dC_s}{dt} = D \left.\frac{\partial C_b}{\partial x}\right|_{x=0} - \varepsilon_s C_s - D^{1/2}\, \varepsilon_b C_b(x = 0) \tag{9}$$

and

$$C_s = \frac{D^{1/2}}{\sigma}\, C_b(x = 0) \tag{10}$$

where $C_s(t)$ is the surface concentration of the solute per unit depth, $C_b(x,t)$ is the bulk concentration, $D(T)$ is the temperature-dependent bulk diffusion coefficient, and ε_s and ε_b are evaporation rates from surface and adjacent bulk layers respectively. The coefficient σ is the surface depletion factor and is proportional to $\exp(-H_{seg})$ where H_{seg} is the heat of segregation. Thus adsorbed species which increase H_{seg} will result in higher surface concentrations of the solute, that is, greater diffusion to the surface.

The diffusion approximation in Eq. (8-10) has been applied with success to systems where the bulk concentration was assumed fixed initially at a constant value.[16] We have now generalized the model to an implant profile which would have a depth dependent initial distribution.[17] Our results show that the implant tends to accumulate at the surface if the diffusion coefficient is large enough. This happens regardless of the size of σ. For larger σ, the implant leaves the surface more quickly, but the largest surface concentration is nearly the same. Thus implants

close enough to the surface or in materials with large enough diffusion coefficients will have significant surface concentrations before equilibrium is reached, even if there is no segregation of the implant at equilibrium.

VII. Size and Heat of Formation Data

Since we have seen that size and heat of formation data are quite useful in determining the constitution and corrosion properties of alloys, we have compiled some of these date for rare earths in Table II. We calculated surface energies from cohesive energy data since there are few measurements in the literature, and we calculated heats of formation for Al and Ni compounds using the Miedema model. We see that there is quite a difference in surface energies so that one would expect Yb, for example, to segregate to surfaces or grain boundaries much more strongly than Ce. However, the much larger volumes of all rare earths with respect to, say, the molar volume of Ni at $6.5\,cm^3$ tends to drive all rare earth impurities to the surface in this solvent. This effect would again be stronger in Yb than in Ce. The heats of formation of Dy, Ho and Er with Ni indicate compounds are probably formed whereas Eu does not form Ni compounds. Also, the rare earths in general tend to order and form compounds more strongly with Al than with Ni.

Table II. Thermodynamic data for rare earth metals. The surface energies are at $0^{\circ}K$ and the heats of formation at room temperature. All energies are in kcal/mole.

M	Molar Volume (cm^3)	Surface Energy	Heats of Formation	
			RNi	RAl
Ce	21.	27.5	-7.4	-20.
αPr	21.	22.3	-7.4	-20.
Nd	21.4	19.3	-8.5	-20.
Pm	20.1		-9.3	-21.
Sm	20.1	12.2	-9.3	-21.
Eu	28.8	10.4	+8.	-12.
Gd	19.7	23.9	-10.	-21.
Tb	19.3	23.5	-10.	-21.
Dy	18.9	17.8	-11.	-21.
Ho	18.9	17.5	-11.	-21.
Er	18.5	19.3	-11.	-21.
Tm	18.1	14.8	-11.	-21.
αYb	24.8	9.0	-.3	-16.
Lu	17.7	27.7	-11.	-21.

VII. Implantation Studies on Ni Alloys

We have initiated a series of implantation studes on Ni-based alloys. The implantations and Auger Analysis were performed by Dr. Keith Legg in the School of Physics. Our first studies were to investigate the effect of implanted Al on the high temperature sulfidation of Ni. The polycrystalline Ni samples were annealed at 750°C for an hour to obtain equi-axed grains and to get rid of dislocations and then were polished down to 1 micron. The implant beam had a primary energy of 100 Kev which created an Al distribution that ranged from the surface to about 1000 Å with a peak at 600 Å and a full width at half maximum of 500 Å. The implant dosage was $2.3\ 10^{17}$ atoms/cm^2 which amounts to an Al concentration of about 40 at% in the implant region. Two samples, one unimplanted (sample A) and one implanted (sample B), were heated in a S ambient at a pressure of about 1 atmosphere at 850°C for 1 hour.

The samples were analysed with scanning electron microscopy (SEM) and x-ray flourescence spectroscopy (EDAX). The SEM photographs are shown in Figs. 6-7. We see that both samples have grains of similar size. The appearance of the surfaces, however, is quite different. Sample A in Fig.6 is flat while sample B in Fig.7 is rumpled as if the grains had grown out. Surprisingly, EDAX shows little difference between the two samples and finds no Al in either case. Analysis of the EDAX spectrum for sample A gives a S concentration of 14 at% at the grain boundary while sample B has 13 at% at the boundary. Since the EDAX signals for S on the grain surface are a good deal smaller, most of the S resides in the grain boundaries with a slightly smaller concentration in sample B.

We next analyzed the samples with a surface sensitive technique, scanning Auger Electron Spectroscopy (SAES). Since EDAX has a range of a few microns, it may not see an Al profile of a few percent concentration in the surface region. However, SAES sees no Al either on the grains or at the boundaries in sample B, even though calculations indicate Al should segregate to the surface. The resolution of the spectra indicates

Fig. 6 Unimplanted Ni after sulfiding.

a. Low mag. showing general grain structure.

b. High mag. showing grain boundary features in arrowed region of a.

Fig. 7 Al-implanted Ni after sulfiding.

a. Low mag. showing general grain structure.

b. High mag. showing grain boundary features in arrowed region of a.

an Al surface concentration of <5% of a monolayer. In agreement with EDAX, the SAES shows a smaller S concentration on the surface and a larger concentration at the grain boundaries. To examine the S depth profile and to see if Al resided under the surface, we next sputtered away about 200 Å of sample B with an Ar beam. Again the SAES showed <5% monolayer of Al, but it also showed removal of S from the grains. A SAES micrograph set for the S peak at 150 eV is shown in Fig. 8. One can clearly see grains of about 60 microns across which are outlined by thick S regions up to 30 microns. However, the SAES shows thicker boundary regions than SEM which indicates that the S profile along the grain boundary must thin out deeper into the sample.

Evidently the Al implant diffuses into the solid at higher temperatures. The addition of O at the surface, to which Al bonds strongly, before raising the temperature may hold the Al in the surface region. The S reduction in sample B indicates that if the Al remains in the surface region, the sulfidation resistance may be improved.

Other implants which would tend to migrate to the surface rather than into the bulk at high temperatures might affect the sulfidation rate. Among the possibilities are Y, Dy or Ce. These are much larger atoms than the Ni substrate and thus would find it energetically favorable to reside at the surface where they could release some of their strain energy. They also bond more strongly to S or O than does Ni so that they would change the chemical nature of the scale. Small amounts of Ce have been shown to increase the adherence of high temperature oxides in Fe-Cr-Al alloys.[15] In fact, a study of the annealing behavior of Ni implanted with Dy ions at a dose of $10^{16}/cm^2$ shows that with heating up to 800°C the implant has migrated to the surface to form a Dy_2O_3 layer.[19]

Fig.8 Scanning Auger micrograph of sulfur-rich regions at grain boundaries of Al-implanted Ni. Magnification is 160x.

IX. Cluster Calculations of Grain Boundary Structure

Even if we can successfully predict the grain boundary concentration, this knowledge tells us little about the effect of an impurity on the boundary strength and adhesion. To address this question we undertook a series of calculations of the microscopic structure of S at Fe grain boundaries. We chose S because of the importance in this work of understanding the effect of S on boundary strength and the adhesion of oxides. We used a molecular cluster model based on the X-alpha approximation to the exchange interaction[20].

To describe the arrangement of atoms at the boundary, we chose a model in which the packing of atoms in metals can be described as the close packing of hard spheres. This is a good approximation for metals. It can be shown[21] that all spacings at the grain boundary in this model for an f.c.c. solid can be built up from combinations of only eight polyhedra called Bernal polyhedra. We chose the 8 vertex polyhedron because it has atoms from both the first and second layers in the boundary region. The structure of the 8 vertex polyhedron is shown in Fig. 9. The atoms at 1,2,3 and 4 are equivalent and describe the two boundary surfaces (atoms 1 and 4 are in one surface, and 2 and 3 are in the other). The atoms 5,6 or 7 and 8 are in the second layer. The procedure entails calculating the self-consistent electronic structure for Fe_8 and Fe_8S and then comparing the results. The S is the center of the polyhedron in the second calculation. Similar calculations have been reported for Ni_8 and Ni_8S[22]. In that case the S was shown to take bonding electrons away from the Ni-Ni bonds resulting in the decrease of bond strength between the first and second layer Ni.

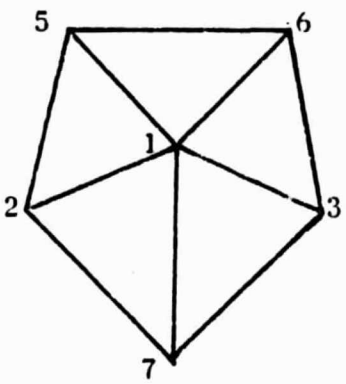

FRONT VIEW

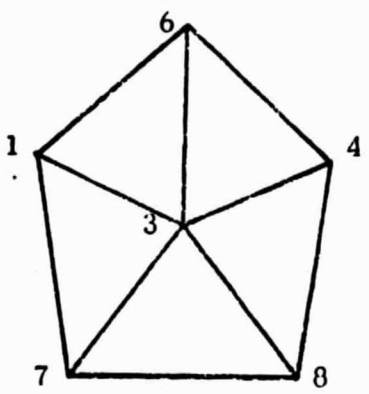

SIDE VIEW

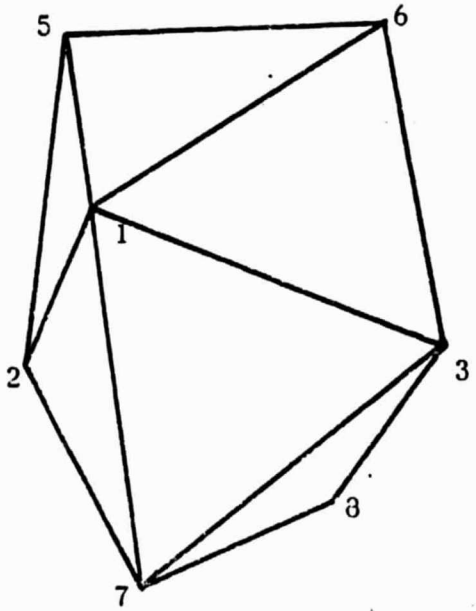

TETRAGONAL DODECAHEDRON D_{2d} SYMMETRY

Fig. 9 Eight vertex Bernal polyhedron for representing an FCC grain boundary.

X. Accomplishments

In the course of this research project, we have established several methods to analyze and predict the composition and behavior of alloys in corrosive environments. We have begun investigations of particular implanted alloys exposed to sulfur at high temperatures and are developing novel methods to look at the alloy behavior. Among our accomplishments are:

- Application of useful models, such as the pair-bonding model, to alloys of interest, such as Ni-Cr-Al.
- Investigation of new effects, such as the surface ordering effect, which may greatly affect the properties of certain materials.
- Correlation of empirical parameters, such as surface energies, heats of solution or volume differences, with the expected behavior of alloy constituents either with or without the presence of O or S. With our models we can use these parameters to get quantitative results for alloy constitutions.
- Improvements of the models to take into account the important effects of long- and short-range ordering and of the kinetics of implant profile changes. This latter effect has not been handled before in a way which takes into account both surface segregation and bulk diffusion effects.
- Investigations of Ni implanted with Al and then exposed to S at high temperature. This work showed what could be obtained with SEMS, EDAX, SAES and other analysis techniques, and the results indicated likely future directions.

References

1. B.D. Sartwell, A.B. Campbell III, B.S. Covino, Jr. and T.J. Driscoll, IEEE Trans. NS-26, 1670 (1979).
2. T. Amano, S. Yajima and Y. Saito, Trans. JIM 20, 431 (1979).
3. A. Kumar, M. Naszallah and D.L. Douglass, Oxid. Met. 8, 227 (1974).
4. G. Kerker, J.L. Moran-Lopez, and K.H. Benneman, Phys. Rev. B 15, 638 (1977).
5. V. Kumar, Phys. Rev. B 23, 3756 (1981).
6. R.E. Watson and L.H. Bennet, CALPHAD 5, 25 (1981).
7. H.H. Brongersma, M.J. Spornaay, and T.M. Buck, Surf. Sci. 71, 657 (1978).
8. S. Mukherjee, J.L. Moran-Lopez, V. Kumar, and K.H. Benneman, Phys. Rev. B 25, 730 (1982).
9. M. Cyrot and F. Cyrot-Lackman, J. Phys. F 6, 2257 (1976).
10. R.E. Watson and L.H. Bennett, Phys. Rev. Lett. 43, 1130 (1979).
11. D.G. Pettifor, Phys. Rev. Lett. 42, 846 (1979).
12. M. Guttmann and D. McLean in Interfacial Segregation edited by W.C. Johnson and J.M. Blakely (American Society for Metals, Metal Park, Ohio, 1977).
13. R. Kikuchi, Phys. Rev. 81, 988 (1951).
14. J.L. Moran-Lopez and L.M. Falicov, Phys. Rev. B 18, 2542 (1978).
15. T. Amano, S. Yajima and Y. Saito, Trans. JIM 20, 431 (1979).
16. G. Rowlands and D.P. Woodruff, Phil. Mag. A 40, 459 (1979).
17. M.W. Ribarsky, Bull. Am. Phys. Soc. 29, 389 (1983).
18. A.R. Miedema, J. Less-Common Met. 46, 67 (1976).
19. R. Andrews, Phil. Mag. 35, 1153 (1977).
20. B.I. Dunlap, J.W.D. Connolly, and J.R. Sabin, J. Chem. Phys. 71, 3396 (1979).
21. M.F. Ashby, F. Spaepen, and S. Williams, Acta Metall. 26, 1647 (1978).
22. C.L. Briant and R.P. Messmer, Phil Mag. B 42, 569 (1980).

APPENDIX

Presented at the 42nd Physical Electronics Conference, Atlanta, Georgia (1982).

Surface Segregation in Ternary Alloy Systems,
M.W. Ribarsky, Georgia Institute of Technology.*

We extend to ternary systems the method of minimizing the total free energy of a crystal with respect to component concentrations in surface and bulk layers in order to calculate surface segregation. In this work we compare results between a pair bonding approach with which one obtains surface free energies using bulk thermochemical data and a continued fraction tight-binding technique suitable for transition metal alloys. With the continued fraction technique, one calculates the electronic Green's function from which one derives the surface density of states. The technique has been applied to random transition metal alloys, and it yields reasonable values fc the surface d-band density of states. For both the pair bonding and tight-binding methods, the free energy minimization condition is a straightforward extension of the condition for binary alloys.[1] For multicomponent systems, one has

$$\frac{\partial F}{\partial x_{iA}} = \frac{\partial F}{\partial x_{iA}} \quad , \; i=1,2,3,\ldots,$$

$$\frac{\partial F}{\partial x_{iB}} = \frac{\partial F}{\partial x_{iB}} \quad , \; \text{etc.....},$$

where F is the free energy, i refers to the surface layer, b refers to a bulk layer, and A,B,C,etc... are the atomic species present. This approach opens the way to studying systems where even trace amounts of a third element can change the surface composition of a binary alloy. For example, small amounts of Al in Ni-Cr alloys will cause the surface oxide to become aluminum oxide rather than chromium oxide. We will give results for some interesting systems for the dependence of surface concentrations on the addition of the third element to binary solutions and also for the effect of chemisorbed species on the surface concentration. We will also discuss the application of this model to grain boundaries. Here one may visualize the grain boundary as resulting from two half-crystals with stepped surfaces "glued" together. The procedure is then to consider separately the Green's function for each half crystal and then consider the effect of interaction across the boundary. Calculations on symmetrical tilt boundaries in s-like metals yield densities of states with sharp structure due to localized boundary staes. The extension of this model to segregation in ternary systems would be important. As an example, Ni, Cr, Mo and Mn alloyed in steels enhance P segregation to dangerous levels causing temper brittleness.

*Supported in part by a grant from NASA-Lewis Research Center.

[1]G. Kerker, J.L. Moran-Lopez and K.H. Benneman, Phys. Rev. B15, 638(1977).

Abstract Submitted
for the March Meeting of the
American Physical Society
26-30 March, 1984

Physics and Astronomy
Classification Scheme
Number 79

Suggested title of session
in which paper should be placed
Ion Implantaion

The Diffusion of Implanted Ions Near Surfaces and Grain Boundaries. M.W. RIBARSKY, Georgia Tech*--At higher temperatures an implant distribution can change greatly from its original profile. We use a diffusion model to investigate the kinetics of the implant distribution in the presence of a surface or grain boundary. The calculations show that the movement and spreading of the implant profile is quite temperature-dependent. The model provides a method for relating the surface and grain boundary enrichment factors to the heats of segregation for these interfaces. Our results show that chemisorbed layers of certain elements or boundary segregation of certain impurities can greatly affect the kinetics of the implant distribution. We also discuss methods for developing a microscopic framework for this model.
*Supported by NASA Grant No. NAG3-255

Please do not schedule on Friday, 30 March.
Please assign to regular program.

Martin W Ribarsky

Martin W. Ribarsky
School of Physics
Georgia Institute of Technology
Atlanta, GA 30332